atmosphere

MDPI

Article

Anthropogenic Photolabile Chlorine in the Cold-Climate City of Montreal

Ryan Hall [1], Oleg Nepotchatykh [2], Evguenia Nepotchatykh [2] and Parisa A. Ariya [1,3,*]

1 Department of Chemistry, McGill University, 801 Sherbrooke Street West, Montréal, QC H3A 0B8, Canada; ryan.hall2@mail.mcgill.ca
2 PO-Laboratories, 609 McCaffrey Street, Saint-Laurent, QC H4T 1N3, Canada; info@po-labs.com (O.N.); evguenia88@gmail.com (E.N.)
3 Department of Atmospheric and Oceanic Sciences, McGill University, 805 Sherbrooke West, Montréal, QC H3A 0B9, Canada
* Correspondence: parisa.ariya@mcgill.ca; Tel.: +(514)-398-6931 (ext. 3615)

Received: 15 July 2020; Accepted: 30 July 2020; Published: 31 July 2020

Abstract: Chlorine atoms play a key role in the oxidative potential of the atmosphere and biogeochemical cycling of selected elements. This study provides a decadal analysis (2010–2019) of chloride ions in $PM_{2.5}$ particles in the city of Montreal, where these are most concentrated systematically in the winter (up to 1.6 μg/m^3). We also herein present the measurement of photolabile chlorine, which includes chlorine-containing compounds (e.g., Cl_2, HOCl, $ClNO_2$, $ClNO_3$, and BrCl) that release chlorine atoms upon interaction with radiation, in urban Montreal, Canada using Cl2-RPGE (Cl2 Reactive Phase Gas Extraction) tubes and quantifying the chlorinated product by GC-MS. Photolabile chlorine in urban Montreal was measured during a discontinuous period primarily in summer 2018 and winter 2019 with a time resolution of 30 min, with concentrations ranging from 3 to 545 ng/m^3 expressed as Cl_2. The reported values are considered lower limits, as compounds such as HOCl and $ClNO_2$ can only be partially converted in the current setup. The largest peak of gaseous photolabile chlorine occurred in the winter, when significant sources of anthropogenic salt are used in snow removal in the city. This coincides with observed chloride ion measurements in airborne particles, implying that anthropogenic salt addition produces photoactive chlorine. The maximum chlorine signal was consistently obtained during the daytime, which is in accordance with the tropospheric radiation profile. Complementary photochemistry laboratory experiments indicated that upon tropospheric radiation ($340 \leq \lambda \leq 400$ nm; UVA), an increase (20–100%) was observed, confirming the formation of Cl atoms from photolabile chlorine compounds. Thus, this portable technique is adequate for Cl atoms and photolabile chlorine-containing compounds upon photolysis using UVA lamps. High-resolution S/TEM and energy-dispersive X-ray spectroscopy (EDS) were used to evaluate collected particle morphology and composition. The behavior of complementary pollutants (O_3, CO, $PM_{2.5}$, and NO_x) was also briefly discussed. We herein discuss the measurement of photolabile halogens within a northern urban metropolitan environment and the impact of anthropogenic sources on chlorine concentrations.

Keywords: atmospheric photolabile chlorine; urban troposphere; anthropogenic chlorine; portable miniaturized trapping technique; gas chromatography mass spectrometry

1. Introduction

The importance of halogens in atmospheric oxidation processes has been observed for decades, notably in stratospheric ozone depletion and tropospheric ozone, some volatile organic compounds (VOC), and mercury depletion in the polar regions [1–6]. Due to the high reactivity of chlorine atoms,

it has been shown that the relative importance of chlorine is comparable to hydroxyl radical (OH) in some regions, including the polar circle during the sunrise. Therefore, chlorine atoms compete with hydroxyl radicals in the tropospheric ozone budget, playing a significant role in urban air quality and the oxidation potential of the lower atmosphere, even at very low concentrations [1–4].

One of the most significant processes for the production of chlorine atoms is the photodissociation of reactive chlorinated compounds. There is a variety of reactive chlorine-containing compounds present in the troposphere, but only a fraction of chlorinated organic and inorganic species in the atmosphere can undergo photolysis and photochemical reactions initiated by atoms in the troposphere. For example, the direct photolysis of chlorocarbons such as CH_3Cl, and $CHCl_3$ has been shown to require UV radiation with wavelengths that are almost entirely absorbed by the ozone layer and do not significantly reach the troposphere [7]. Howeer, the photolysis of Cl_2 as well as compounds such as HOCl, $ClNO_2$, $ClNO_3$, and BrCl readily occurs in the troposphere and releases chlorine atoms upon tropospheric photolysis [1,3,8]. These species can be referred to as photolabile, as they undergo change when exposed to particular wavelength ranges of radiation. Chlorine-containing species such as $ClNO_2$ are of particular relevance when discussing chlorine chemistry within an urban environment, as it is produced under urban polluted conditions due to the enhanced interaction with compounds such as NO_x [9–12].

Oceans containing saltwater cover the majority of the Earth's surface, and natural halogens have been observed over salt-rich domains such as oceans, salt lakes, and coastal regions [1]. However, various industrial activities produce significant amounts of anthropogenic halogens directly and indirectly. Recent reports show a significant increase of chlorine-containing emissions, such as chloroform, in some developing countries [13]. It has been suggested [13] that the increase in anthropogenic production (e.g., agriculture, chloralkali, chemical, etc.) of chlorinated methane in Chin, is such that it can compensate for the decrease of chlorofluorocarbons, which destroy ozone. Thereby, an urgency to understand diverse sources of anthropogenic chlorine has renewed.

Previous measurement of atmospheric chlorine compounds has primarily been taken in polar, marine, and coastal regions using chemical ionization mass spectrometry (CI-MS) or atmospheric pressure chemical ionization mass spectrometry (APCI-MS), which allowed for the quantification of chlorine species in real time [1]. These regions have been the primary focus due to the elevated levels of atmospheric halogens. While there have been some more recent studies of halogen chemistry in cities [1–3,10,11,14], there are still gaps in our knowledge of chlorine chemistry in cold-climate polluted cities.

The aim of the current work is twofold: (1) long-term measurement of chloride in airborne particles; (2) measurement of photolabile chlorine to evaluate coupling between the chloride ions and the generation of photolabile chlorine species that release chlorine radicals by using the photolabile measurements. The observed increase in atmospheric reactive chlorine is particularly relevant to cold-climate cities such as Montreal, which receives approximately 2.3 m of snow per year. The amount of snowfall is relevant because it dictates the amount of de-icing road salt, a potentially significant source of chlorine, that is needed. We strived to explore the impact of the addition of anthropogenic chloride to form photolabile chlorine species and thus alter the oxidation chemistry. We have analyzed 10 years of data of chloride ions in the city of Montreal and measured photolabile chlorine in a northern urban environment using a novel particle interface coupled to gas chromatography-mass spectrometry. A series of measurements were performed in the City of Montreal in the field and in the lab under controlled conditions to evaluate the level of reactive chlorine compounds in the city and the impact of anthropogenic winter activities in particular. Such results are of significance in urban air quality, particularly in cold cities, where the addition of salt is ubiquitous during cold seasons for melting snow/ice.

2. Experiments

This section provides information on data provided by the National Air Pollution Surveillance Program (NAPS) and the development of the particle-based sorbent material for photolabile chlorine collection and measurement during this work.

2.1. Observational Data from the National Air Pollution Surveillance Program (NAPS)

NAPS is a program designed to provide accurate long-term data across Canada for monitoring and assessing ambient air quality. The program utilizes data provided by numerous regional government research organization partners located in different cities and regions of Canada and makes the data publicly available after rigorous data validation and quality control. The validated NAPS data is available in the public domain [15]. Note that there is a delay of about one year for the validation and release of the data.

NAPS was used to provide data for O_3, NO_x, CO, and Cl^- collected from airborne $PM_{2.5}$ particulates. O_3, NO_x, and CO are all measured constantly in real time, and the data are provided in hourly averages for a total of 24 data points per day in ppb. O_3 is measured using a UV-photometric Analyzer (Thermo 49i), NO_x (NO + NO_2) chemiluminescence is measured using a NO–NO_2–NO_x Analyzer (Thermo 42i), and CO is measured using a trace level enhanced gas filter correlation analyzer (Thermo 48i). Cl^- data is provided as one of the analytes detected from the analysis of $PM_{2.5}$ particulates using a Met One SuperSASS-Plus Sequential Speciation Sampler. The sampling frequency is 1 every 3 days, for a period of 24 h. The sample is collected on a Teflon filter, processed with water extraction, and analyzed with ion chromatography in order to obtain Cl^- in $\mu g/m^3$. Data were used from NAPS site ID 50,115 located at 45°30′05.5″ N 73°34′27.5″ W approximately 300 m from the sampling location at McGill and changed location in 2016 to 45°30′43.9″ N 73°34′00.6″ W approximately 1 km from the sampling location at McGill. The new sampling location is relevant for the comparison with this work's measurements.

2.2. Materials

In the current study, Cl2-RPGE tubes were used to sample chlorine reactive species from the air. The Cl2-RPGE tubes (Reactive Phase Gas Extraction) were purchased from PO-Laboratories, Montreal, Canada. The Cl2-RPGE tubes are packed with a proprietary material that provides the effective adsorption of chlorine with its subsequent transformation to a single product, which is an organic chlorinated compound that can be detected by GC-MS or HPLC. An image of a Cl2-RPGE tube is shown in Figure S1, Supplementary Information. Other materials are ultra-high purity grade helium gas as a mobile phase, purchased from AirLiquide, Pointe-Claire, Canada and HPLC grade acetone (Sigma-Aldrich, Oakville, ON, Canada). The internal standard used for these experiments was 0.1% fully deuterated naphthalene (D8) (Sigma-Aldrich) in acetone.

2.3. Analysis of Cl2-RPGE Tubes by GC-MS

In this study, we used GC-MS detection method utilizing MS single-ion mode for the ion m/z = 178, which corresponds to the organic chlorinated compound of interest, formed in the Cl2-RPGE tubes during sample collection. Although the chemistry of the Cl2-RPGE tube is not disclosed, we fully validated the Cl2-RPGE tube–GC-MS method. The method provided a required detection limit (0.3 ppt), quantitation limit (1 ppt), range (1–200 ppt), excellent repeatability, stability, and quadratic linearity; please refer to the Supplementary Information section. The signal versus concentration curve is quadratic, and this is typical for the electron-impact ionization mass spectrometry, because the efficiency of ionization is related to the analyte concentration in the MS ion source.

Sample preparation: The Cl2-RPGE tubes, used for chlorine sampling as described further below, were loaded with 200 µL of acetone. A small amount of air pressure was used to push the acetone through the Cl2-RPGE tube, and the obtained liquid was collected into the 2-mL centrifuge tube.

The acetone extraction step is once again repeated, obtained liquid is collected into the same tube, and 20 µL of internal standard solution (0.1% fully deuterated naphthalene (D8) in acetone) added into the tube. The tube was vortexed, and finally, 2 µL of the sample containing liquid was injected in GC-MS.

GC-MS measurements were performed using a Thermo-Finnigan Trace-GC Ultra (Thermo Ficher Scientific, Mississauga, ON, Canada) coupled with a Polaris-Q MS (Thermo Fisher Scientific, Mississauga, Canada). The column was Agilent J&W DB-FFAP (Agilent Technologies, Mississauga, Canada) with a length of 30 m, a diameter of 0.250 mm, and a film thickness of 0.25 µm. Helium gas was used as the mobile phase with a gas velocity of 25 cm/s.

The oven temperature program was as follows: an initial temperature of 100 °C was held for 0 min, followed by a temperature ramp of 15 °C/min until a final temperature of 220 °C, which was held for 17 min. The inlet temperature was 230 °C, and the transfer line temperature was 220 °C. The ion source temperature was 150 °C with an ion range selected of 100−200 m/z.

2.4. Blank Experiments with NaCl and HCl

The Cl2-RPGE tubes were exposed to known concentrations of HCl and NaCl in order to assess the effects of these compounds on the Cl2-RPGE tubes, and if there were a signal generated that would influence atmospheric sampling results. HCl and NaCl aerosols are of interest, as these chlorine-containing aerosols will also be collected in the Cl2-RPGE tubes during atmospheric sampling. Solutions of 2 different concentrations were made for both compounds: a very concentrated and a dilute solution at 0.05 M and 1×10^{-6} M, respectively. These solutions were placed in a 30 mL syringe (BD) and placed on a syringe pump. The syringe was connected to a nebulizer, which sprayed the nebulized solution though 2 diffusion dryers. The gas used to enable nebulization was compressed dry air. During the experiments, the syringe pump pumped the solutions at a rate of 0.25 mL/min, and the compressed gas pressure was held at approximately 50 psi. Before connecting the Cl2-RPGE tubes to the outlet of the diffusion dryers, we first used a TSI Nanoscan SMPS 3910 (Scanning Mobility Particle Sizer) (TSI Incorporated, Shoreview, MN, USA) and a TSI OPS 3330 (Optical Particle Sizer) (TSI Incorporated, Shoreview, USA) to measure the aerosol output of the setup, for both the particle size distribution and particle count. After the Cl2-RPGE tubes were connected, the gas was adjusted such that the flow through our sampling Cl2-RPGE tubes was at approximately 1 L/min. The actual flow rate was measured using a TSI mass flow meter. The sample time for all tests was 30 min.

To further characterize the Cl2-RPGE tubes, we tested to see if gaseous HCl would pass through without reacting with the Cl2-RPGE tube material. The setup for this experiment involved a sealed vessel containing a solution of 0.05 M HCl. A cylinder of compressed dry air was connected such that bubbled air passed through the solution, passing through connected Cl2-RPGE tubes and carrying a large amount of HCl, with a sample time of 30 min. This concentration was chosen as an extreme, as it is far beyond atmospheric levels. If there is still no signal as a result of only reacting with HCl gas, this confirms that HCl gas does not directly interfere with the measurement of photolabile chlorine-containing compounds.

2.5. Photolabile Chlorine Measurements, Downtown McGill Campus

Experiments were conducted at McGill University by drawing ambient outdoor air through the sorbent material devices. The outdoor air was pulled in through a 50 cm length of 1/8 in outer diameter × 0.030 in wall PFA Teflon tubing to where the devices are located within the laboratory. A set of 3 devices was set up in parallel during these experiments, such that all sampling would be done in triplicate. Each device was connected to an Omega rotameter to roughly control the flow rate through each device, while a TSI Mass flow meter was used to determine precise flow rates during each sampling period, with all sampling performed at 1 LPM for 30 min. A SKC Vac-U-Go Area Sampling pump (SKC, Eighty Four, PA, USA) provided the vacuum for this setup. The sampling setup is shown in Figure S3, Supplementary Information (SI).

Air samples were taken during a discontinuous period from March 2017 to May 2019, primarily from May 2018–August 2018 and December 2019–April 2019. These samples were taken to assess the usability of the particle-based sorbent method for use on environmental atmospheric samples. To evaluate the daily photochemical variation affecting photolabile concentration, we have taken samples at various times throughout the day and night. The results of these tests showed the total effect of pollution from daily activity, as well as solar radiation on the Cl_2 concentrations detected. Blank runs were performed by passing dry compressed air through the system and measuring any small amount of residual chlorine collected on the tubing and Cl2-RPGE tubes, which was not significant.

Trends of photolabile chlorine concentrations are observed at peak daylight hours and compared to hours in the middle of the night. This pattern was observed systematically throughout all data sets, which hinted to photochemical processes. Hence, the experimental photochemistry was designed to explore qualitatively whether daytime peaks and nighttime low photolabile chlorine values are due to solar radiation-initiated photochemical reactions. To mimic field observation at low tropospheric conditions, we place tubing in an enclosed photochemical chamber, which is basically a ventilated dark wooden chamber that contained 4 Hitachi 15 W F15T8/BL Black Lights, which emit a relatively broad UV-A radiation ($340 \leq \lambda \leq 400$ nm, optimized for 370 nm). Such systems have often been used in field experiments for photochemical reactions of gaseous and water samples [16,17] to mimic the continuous weak UV radiation that approaches the lower troposphere, which happens to be also an appropriate range for the photolysis of Cl_2. These broad band UV-A lamps were used because they enable the photolysis of different compounds within the wavelength range, in a similar manner to solar band radiation.

Ultra-violet (UV) radiation exposure experiments exhibited similar patterns to observed diurnal data on measured chlorine concentrations, confirming that this behavior is likely due to the effects of solar radiation. The presented photolysis experiments and the corresponding setup were utilized for the purpose of qualitatively observing an increase in measured chlorine corresponding to radiation exposure. They are not intended for quantitatively determining photolysis parameters.

The particle-based devices being used to test the effects of UV radiation are now connected immediately at the exit of a 150 mL cylindrical Pyrex cell in order to allow significant exposure of the incoming air to the UV radiation before immediately passing through the sorbent material. The residence time of the vessel is approximately 1 s. All samples collected were taken at a flow rate of 1 LPM, and samples were typically collected over a period of 30 min unless stated otherwise for testing purposes. Breakthrough of Cl_2 was not observed under these conditions. Blanks for the UV exposure experiments involved passing dry compressed air through the system to observe any residual chlorine produced from the walls of the vessel.

Under the current experimental conditions, species such as $ClNO_2$, $ClNO_3$, HOCl, and BrCl can only be partially photolyzed. UV B lamps would need to also be used, as these species are more efficiently photolyzed at higher energy wavelengths. This can be demonstrated in Figure S4 by comparing the wavelengths of the UV lamps in this study to the wavelengths of absorption for selected relevant molecules. Figure S5, Supplementary Information, shows a solar irradiance spectrum as reference for relevant wavelengths. A more transmissible material would also be needed for the cell, such as quartz, in order to allow a wider range of UV wavelengths as well. The UV experiments are used to confirm if the Cl2-RPGE (Cl2 Reactive Phase Gas Extraction) tube material reacts with released chlorine atoms and to identify the release of chlorine atoms from photolabile compounds that were otherwise not as reactive toward the Cl2-RPGE tube material. Hence, the extent of the photolytic conversion of chlorine-containing photolabile compounds is a factor that should be studied and enhanced in the future.

2.6. Technical Details and Technique Validation

Figure S2a, Supplementary Material, shows a representative calibration plot for the GC-MS method for the analysis of sorbent materials that have been loaded with a known amount of Cl_2.

Calibration data points are the ratios of the peak area of the target chlorinated molecule compared with the peak area of the internal standard (0.1% fully deuterated naphthalene (D8)). The detection limit of this method depends on a variety of factors. The practical equipment constraint is that if the amount collected on the material produces a peak that is small enough to be buried in the instrument background noise, quantitation is not possible.

The sampling time should be as short as possible while still producing a strong enough signal, such that the averaged chlorine concentration is not affected by weather changes during the sampling period, such as wind direction. To estimate the amount of chlorine that must be collected on a given device to produce a quantifiable signal, the limit of quantification (LOQ) is calculated based on a signal-to-noise ratio (s/n) of 10, whereas the limit of detection (LOD) is calculated based on a s/n of 3. The LOQ and LOD are estimated to be 3 ng/m^3 (1 ppt) and 0.9 ng/m^3 (0.3 ppt) using this method under our current sampling conditions of 30 min at 1 LPM. Additional information regarding method accuracy, repeatability, and intermediate precision is provided in Tables S1–S7 in Section S2, Supplementary Information.

Selected samples were kept in sealed containers under refrigeration and stored for a significant period before preparing the sample and running with GC-MS. This aging period was up to a week in length. Comparison with concurrently sampled Cl2-RPGE tubes, which were not stored as long, demonstrated that under appropriate storage conditions, comparable results are obtained with or without aging. A more detailed summary of the specific factors affecting uncertainty is available in Supplementary Information S5.

2.7. High-Resolution Scanning Transmission Electron Microscopy (STEM) Imaging with Energy-Dispersive X-ray Spectroscopy (EDS)

The particles collected from Cl2-RPGE tubes that were loaded from atmospheric sampling were placed on a 400 mesh Cu grid from SPI (SPI supplies, West Chester, PA, USA). Placing the grid in contact with the particles allows for a sample observable with STEM to remain on the grid surface. The TEM grids for our samples were analyzed using a high-resolution FEI Tecnai G2F20 S/TEM microscope with a field emission gun (FEI Company, Hillsboro, OR, USA). The field emission gun transmission electron microscope (FEG-TEM) has an operating voltage with a range of 50 to 300 kV. The gun's properties of high brightness and high coherency allow for large electron probe currents to be focused on nanometer-sized areas of the target object being studied. The gun's capabilities include energy-dispersive X-ray spectroscopy (EDS) for elemental composition determination, STEM for imaging and mapping, and a CCD (charge-coupled device) camera that allows magnification of thin samples (<500 nm) up to >1 million times.

3. Results

3.1. NAPS Observational Data

NAPS observational data show trends in atmospherically relevant gaseous species in Montreal during a 10-year period leading up to and including our trap-sampling period. Significantly, the NAPS data also provide chloride measurements obtained from $PM_{2.5}$ particulates collected. Figure 1 shows the trends during 2010−2019 for chloride, O_3, NO_x, CO, and $PM_{2.5}$ obtained from NAPS.

Data from each season were averaged in order to observe the seasonal averages of each analyte. Figure 2 summarizes the seasonal averages for chloride, O_3, NO_x, CO, and $PM_{2.5}$. It is of importance to note the significant increase in chloride during the winter season, showing potential evidence for the impact of anti-ice measures taken by the city during winter, generally agreeing with previous studies that demonstrated significant increases in chloride in winter due to de-icing measures [18–20]. While the trends of chloride agree well with a winter maximum, it must be made clear that not all measured chloride or chlorine atoms, in the case of this work's measurements, are from the salt addition. Reactive chlorine species are still also generated either directly or indirectly through other

surface reactions and regular urban processes such as industrial activity [20]. O_3 measurements show a maximum signal in the spring, with a minimum in fall. NO_x and CO both show a maximum in the winter season followed closely by the fall values, with a minimum in the spring or summer, depending on the year. These co-pollutants indicate that there may be a role of the boundary layer height in modifying atmospheric concentrations due to peak values of NO_x and CO in winter, but it would not be able to completely account for the significant increase in chloride ions. Figure S6, Supplementary Information, demonstrates the possible influence of boundary layer height by showing the ratio of a given measured species over CO. Other studies have demonstrated the seasonal increase in chloride and the urban chlorine atom precursor $ClNO_2$ in winter, with the significant increase being mostly due to salt additions to roads [11,19]. An additional plot of the result time series of O_3 and NO_x concentrations is shown in Figure S7, Supplementary Information, to demonstrate that this value also peaks in winter for each year shown as further support for an increase on $ClNO_2$ in winter. Figure S8, Supplementary Information, demonstrates possible impact of boundary layer height on the product plotted in Figure S7.

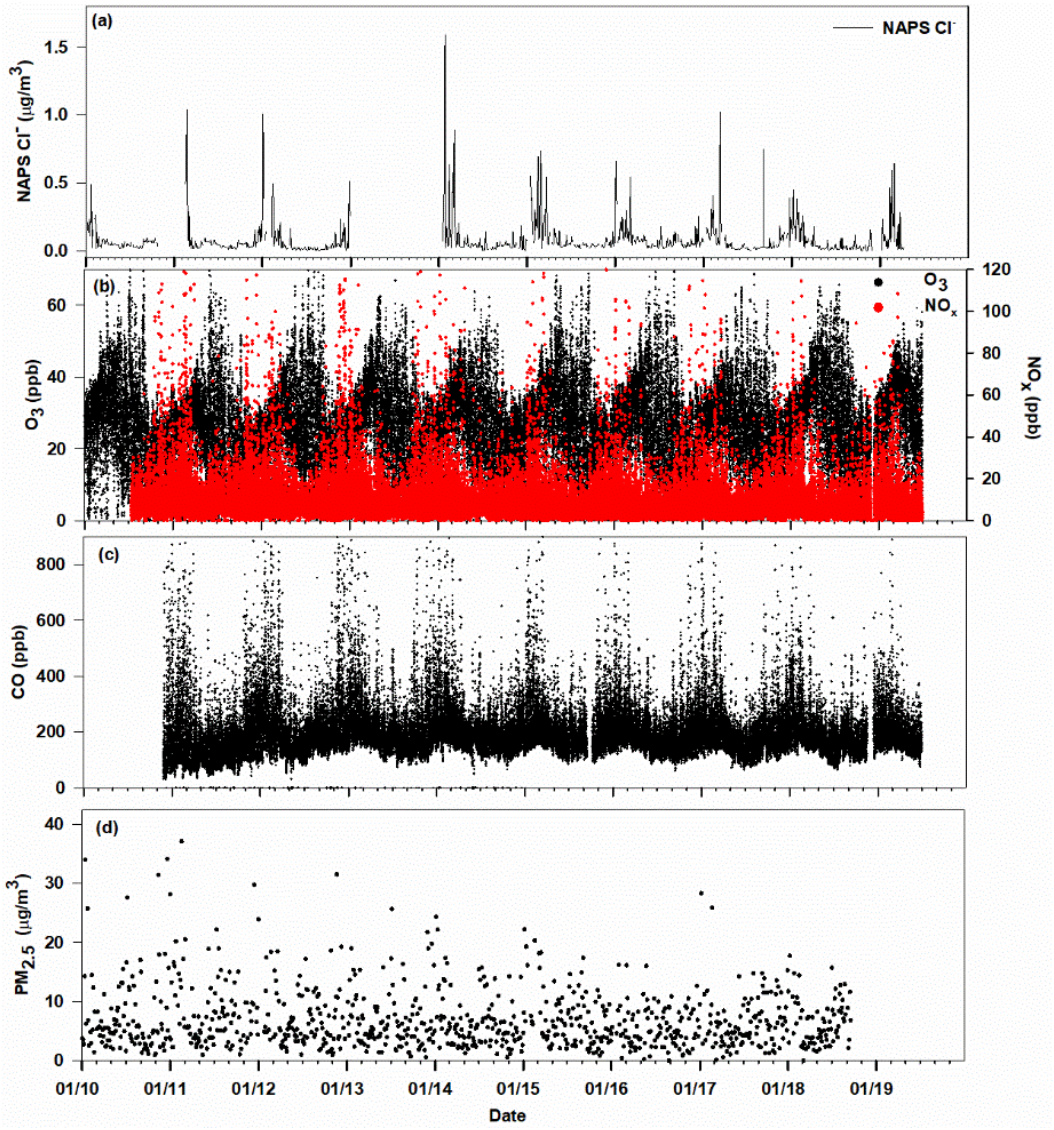

Figure 1. National Air Pollution Surveillance Program (NAPS) data showing 10-year trends for (**a**) Cl^- from $PM_{2.5}$ integrated measurements, (**b**) O_3 and NO_x hourly averages, (**c**) CO hourly averages, and (**d**) $PM_{2.5}$ 3-day integrated sampling measurements. The NAPS site location changed in 2016.

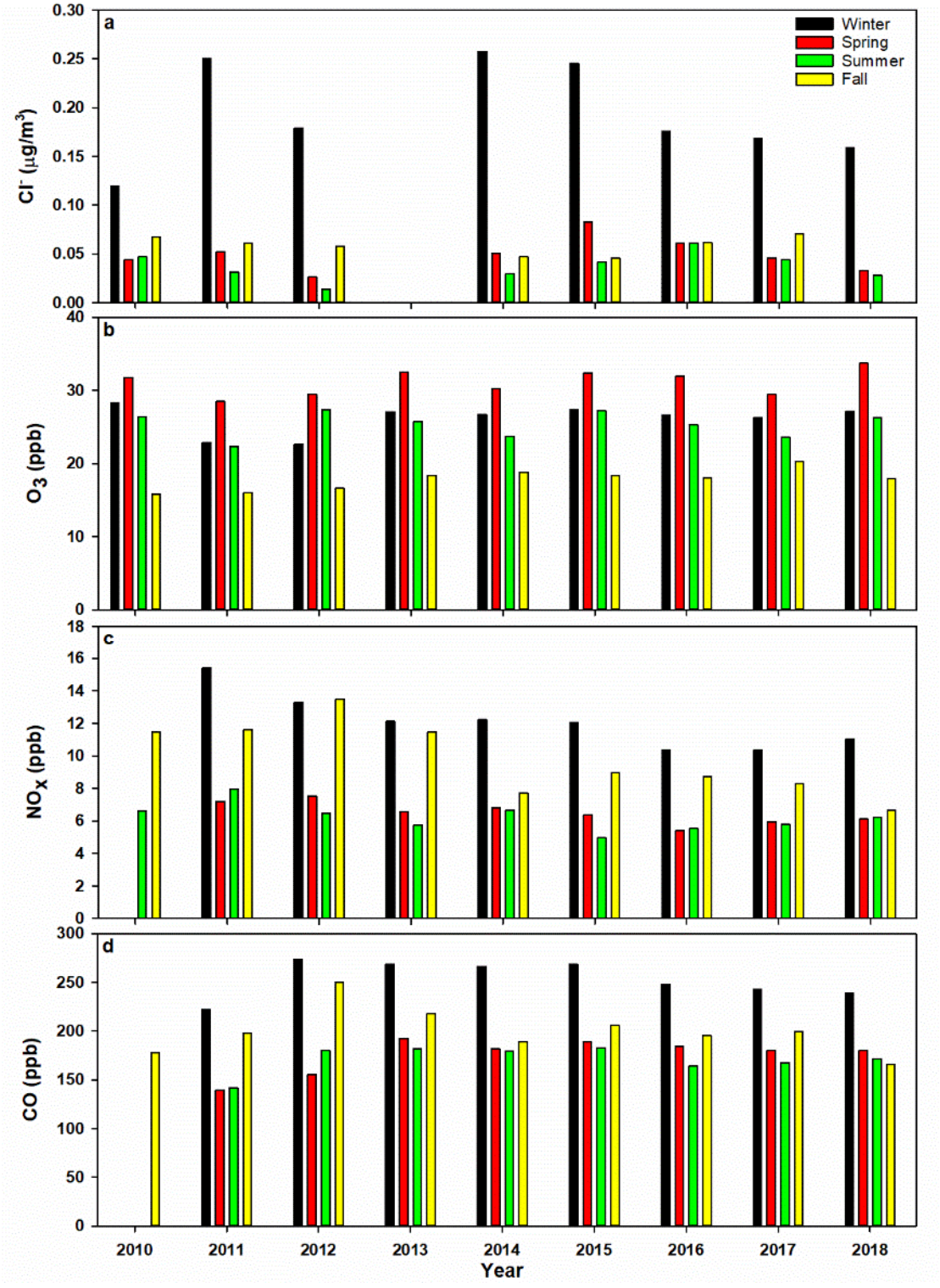

Figure 2. NAPS data showing seasonal (**a**) Cl^- averages from $PM_{2.5}$ particles, (**b**) O_3 averages, (**c**) NO_x averages, and (**d**) CO averages from 2010 to 2018. Winter is counted from December to March, Spring is counted from March–June, Summer is counted from June to September, and Fall is counted from September to December. The winter for a given year is including the December period from the end of the previous year. For example, winter in 2012 is including December 2011. The NAPS site location changed in 2016.

3.2. Measurement of Photolabile Chlorine from Downtown McGill Campus

The Cl2-RPGE tubes were used to sample urban Montreal air for GC-MS analysis. The target ion was at 178.10 m/z, which typically had a retention time of 6.52 min in the chromatogram. Positive identification of the chlorinated product was made by the formation of the target ion peak as it is formed after reaction of the Cl2-RPGE tube material with the sampled chlorine and is not present in the starting material. Representative chromatograms for a calibration standard and a sample are provided as Figures S9 and S10, Supplementary Information. Blank measurements with compressed dry air are taken for eliminating any measured chlorine that may be trapped during storage, transport, or any handling other than during active sampling. All measurements taken are blank subtracted.

Figure 3 shows the diurnal time series of measured photolabile chlorine concentrations taken during the period from March 2017 to May 2019. These samples were taken to demonstrate the usability of the method and to produce the expected trends in chlorine concentrations. It is generally observed that over the sampling period, the concentrations measured during daylight hours are elevated as compared to concentrations measured during night hours. This is particularly emphasized between the hours of 11:00 and 15:00. It must be noted that this trend is observed even though our current sampling setup may result in the loss of a significant fraction of chlorine atoms in the inlet. While the current setup has this limitation that does not allow a full quantification of chlorine atoms, the diurnal trend is still observed. This trend is as expected due to both increased pollution during business hours, but most importantly due to the photolysis of halogen-containing compounds when exposed to UV radiation. UV-A radiation ($340 \leq \lambda \leq 400$ nm) is of relevance to the lower troposphere. While it is known that compounds such as $ClNO_2$ are produced during night hours, we do not expect to efficiently collect them without direct UV exposure, as these compounds are not likely to fully react with the Cl2-RPGE tube material due to the slower reaction rates and steric effects. There may also be secondary reactions occurring in the inlet tubing that produce reactive chlorine compounds, but any amount of reactive chlorine produced under such conditions was not significant above the LOD or did not react with the Cl2-RPGE tube material.

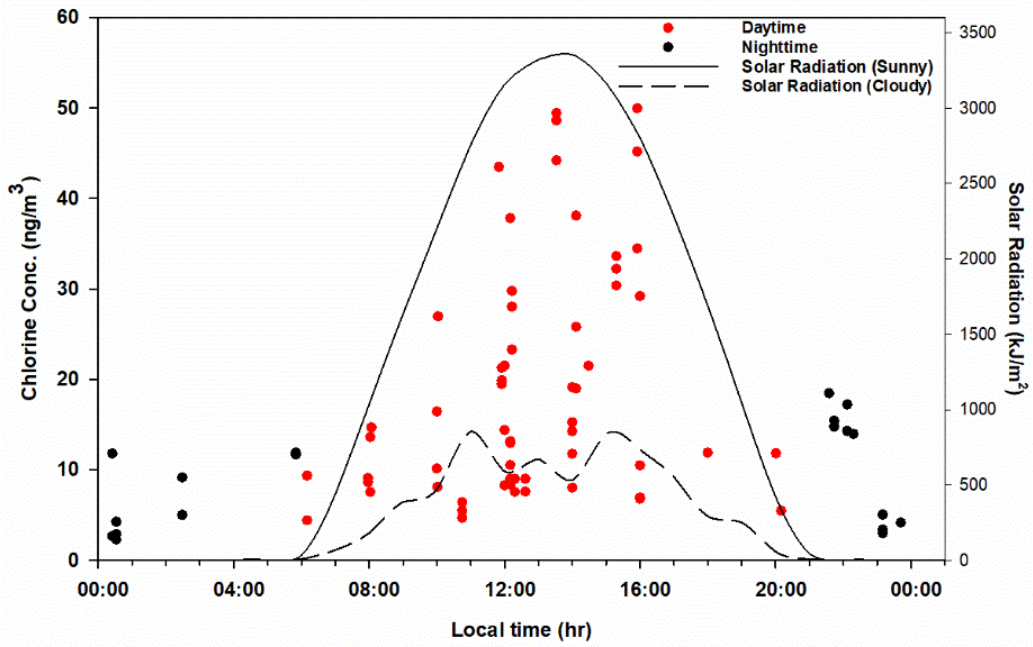

Figure 3. Diurnal time series of measured photolabile chlorine concentrations taken during July 2017, May–June 2018, and March–April 2019 showing the 24-h trend observed, indicating the photolysis of halogenated compounds from sunlight exposure. Recorded solar radiation from a sunny day (12 June 2018) and an overcast day (14 June 2018) in Montreal are shown for reference.

Figure 4 shows the direct comparison of samples taken during the daytime and nighttime of the same days. Daytime samples were taken during peak daylight hours, and nighttime samples were taken at least 4 h after sundown. A paired *T*-test shows a statistically significant difference between day (M = 36 ng/m^3, SD = 9.4 ng/m^3) and night (M = 18 ng/m^3, SD = 7.7 ng/m^3) samples, with a two-tailed p-value of <0.001.

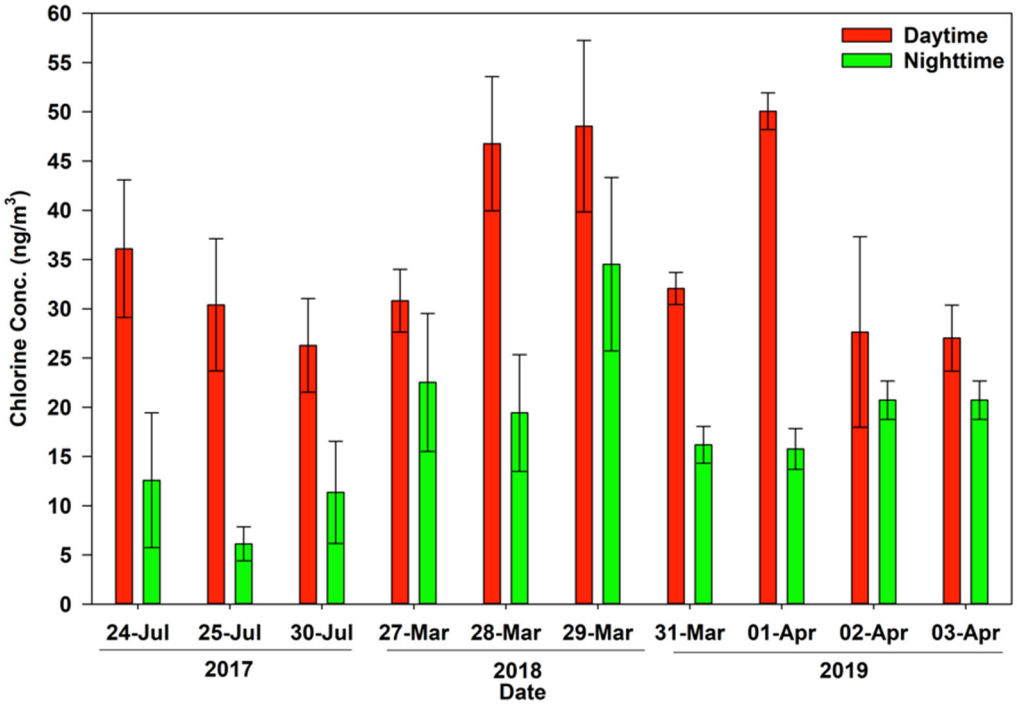

Figure 4. Direct comparison of samples taken during peak daytime and nighttime hours for various days during the experimental sampling period.

3.3. UV Exposure Comparison

In addition to regular sampling periods, selected samples were exposed to UV-A radiation during the sampling process. This allows for the measurement of additional chlorine atoms released from photolyzable compounds that would otherwise not as efficiently react with the sorbent material. It must be noted that without UV B (280 nm−315 nm) radiation as well, a significant portion of photolyzable compounds such as $ClNO_2$ may not undergo complete photolysis. These results demonstrate that the chlorine atoms released from photolyzed compounds can be collected by reacting with our Cl2-RPGE tubes, but further modification of the setup will be needed for complete photolabile compound detection. Figure 5 shows the increase in measured chlorine concentrations of UV-exposed samples relative to the coinciding samples kept in the dark, which were sampled in parallel. A paired *T*-test shows a statistically significant difference between UV-exposed (M = 49 ng/m^3, SD = 16 ng/m^3) and dark (M = 27 ng/m^3, SD = 12 ng/m^3) samples, with a two-tailed p-value of <0.001.

The significant difference between the UV-exposed and dark samples indicates the presence of photolabile chlorine compounds that otherwise either did not react with the Cl2-RPGE tube or had a slow enough reaction rate with the Cl2-RPGE tube material that not all of the photolabile species was collected. This indicates that with an appropriate setup utilizing a wider range of UV wavelengths (not only UV A) and a cell made of more transmitting material, such as quartz, we may use this Cl2-RPGE tube material to measure a more complete range of photolabile compounds. The currently measured values identify a lower limit to what is potentially a much higher amount of photolabile chlorine-containing species.

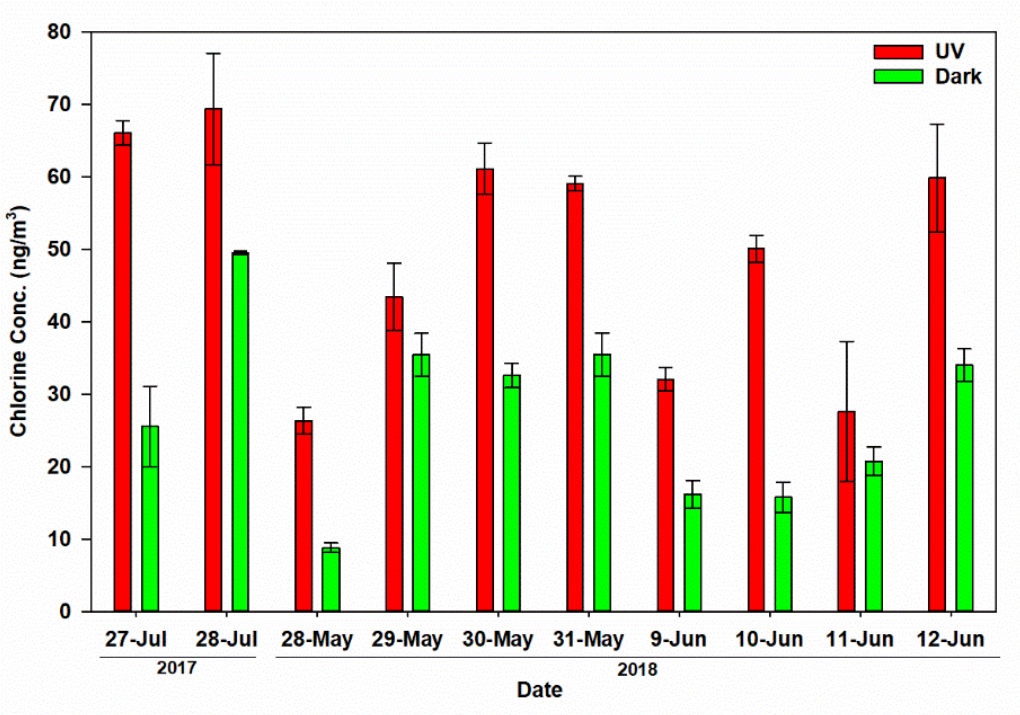

Figure 5. Comparison of UV-A exposed samples to concurrently sampled dark samples. Samples included are from multiple sampling periods, during daylight hours between 11:00 and 16:00.

3.4. Results of NaCl and HCl Blank Experiments

When Cl2-RPGE tubes were exposed to concentrations of gaseous HCl that were much higher than atmospherically realistic values, there was still no signal generated above the level of background noise. This confirms that the measured values of chlorine are not including gaseous HCl, which does not react with the Cl2-RPGE tubes during sampling. HCl is not photolyzed by tropospheric UV, and thus it is not measured directly with this Cl2-RPGE tube-based method. However, it must be mentioned that for the previously described UV exposure experiments, there may be a possible indirect interference by trace gases such as HONO. HONO can be photolyzed and produce OH, which can react with HCl to produce Cl and H_2O. This interference in the UV experiments will need to be further studied and even more so for O_3 in the presence of UV B light and humidity.

In a similar manner, HCl aerosols were tested and did not produce a detectable signal above background noise. However, this is only true when the experiments produced a particle count of approximately 1×10^4 cm^{-3}. When the particle counts measured with the SMPS and OPS were significantly higher than what can be expected to exist in the atmosphere, beyond the ability of the instruments to measure ($>1 \times 10^6$ cm^{-3}), elevated signals are detected. This is likely because water droplets build up in the Cl2-RPGE tube during both concentration tests. Once there is too much water present in the Cl2-RPGE tubes, the dissolved HCl, and therefore the Cl^- ions, may react with the trap surface through aqueous-phase chemistry with the Cl2-RPGE tube material. In the case of the second test, there is a much higher concentration of Cl^- ions present in the water on the Cl2-RPGE tubes. This is also a main reason why the measurements taken in the current work were not taken during periods of high precipitation, in addition to the general washout effect that rain may have.

When the aerosol experiments were performed with NaCl, the behavior was very similar to that of HCl aerosols. As NaCl also dissolves in water to release Cl^- ions, an immeasurable particle count of $>1 \times 10^6$ cm^{-3} for NaCl aerosols will produce the same effect as with HCl. Most importantly, when the particle counts were kept at approximately 1×10^4 cm^{-3}, there was no detectable signal above the background noise. In summary, the characterization experiments showed that HCl gas, HCl aerosols, and NaCl aerosols do not significantly impact measurements under experimental conditions. This may

be an expected result when assessing the oxidation state of chlorine in these compounds, which is −1. An oxidation state of +1 is expected for chlorine in order for electrophilic addition to an activated aromatic to occur. It must be noted that while a particle count of 1×10^4 cm^{-3} may be common in some polluted metropolitan cities, this particle count consists of many different aerosols and particles. In the case of these tests, all particles measured were generated from a solution of HCl or NaCl. Therefore, even the lower concentration tests contain much higher HCl or NaCl aerosols than would normally be present in the atmosphere.

3.5. Morphology and Elemental Composition of Particles

S/TEM and EDS measurements were taken to characterize the morphology and, most significantly, the elemental composition of particles that have been collected during sampling to show the presence of chlorine-containing particles. The particles analyzed were taken from Cl2-RPGE tubes that were used to sample for 30 min at 1 LPM but before any extraction for GC-MS was performed. The 3 particles analyzed below are selected ambient particles that were collected during measurements and not coated sorbent particles, which have a much larger diameter in comparison. These particles were selected due to the presence of halogens, but there were several other types of particles observed. It must be stated that the analyzed particles are not the majority of particles present and are in the minority under our experimental conditions and analysis. In addition, due to the nature of electron microscopy, there are particles present that we did not directly observe, which may have contained elements of interest.

S/TEM images depict the existence of several irregularly shaped particles including nanoparticles, along with other nano-size (100 nm to 1 microns) and micron-size particles, which have been removed from the loaded sorbent after sample collection. While the Cl2-RPGE tubes are composed of particles, they will also collect a small portion of airborne particles during the sampling process. These airborne particles may also contain chloride, but they do not impact measurements. This is demonstrated in the aerosol experiments by showing that an atmospherically relevant concentration of chloride in HCl and NaCl aerosols does not produce a measurable result. Therefore, the chlorine-containing particles can be considered to have no impact on measured results. The elemental composition of the measured particles as determined by EDS is predominantly C, N, O, S, and Si with Cl, Br, K, Na, F, Mg, Ca, and other minerals present. Figure 6a,b shows a rigid particle with the presence of soot, which is based on the chain-like structures attached to the main body of the particle. The elemental composition also demonstrates the presence of chlorine.

The presence of particles composed of the elements Si, O, C, Mg, and Ca such as in Figure 6c,d, appear to indicate the presence of calcium carbonate-like structures, which may arise from construction and road dust near the sampling site, although Si, O, and C are present in the sorbent materials as well. A chlorine peak in EDS is clearly present in Figure 6c,d, although this may arise from the uptake of chloride precursor gases, such as HCl, by the Ca-containing compounds. EDS also identified the presence of bromine, as shown in Figure 6e,f. The detection of bromine indicates the presence of atmospheric bromine species, which are typically at much lower concentrations than chlorine species. The Br detection by EDS may indicate that the concentrations of bromine species may be within the range for the current methodology to measure quantitatively, upon modification of the sampling procedure. Some such modifications would include minimizing the inlet to reduce any possible losses, increasing the sample time and increasing the sample flow rate.

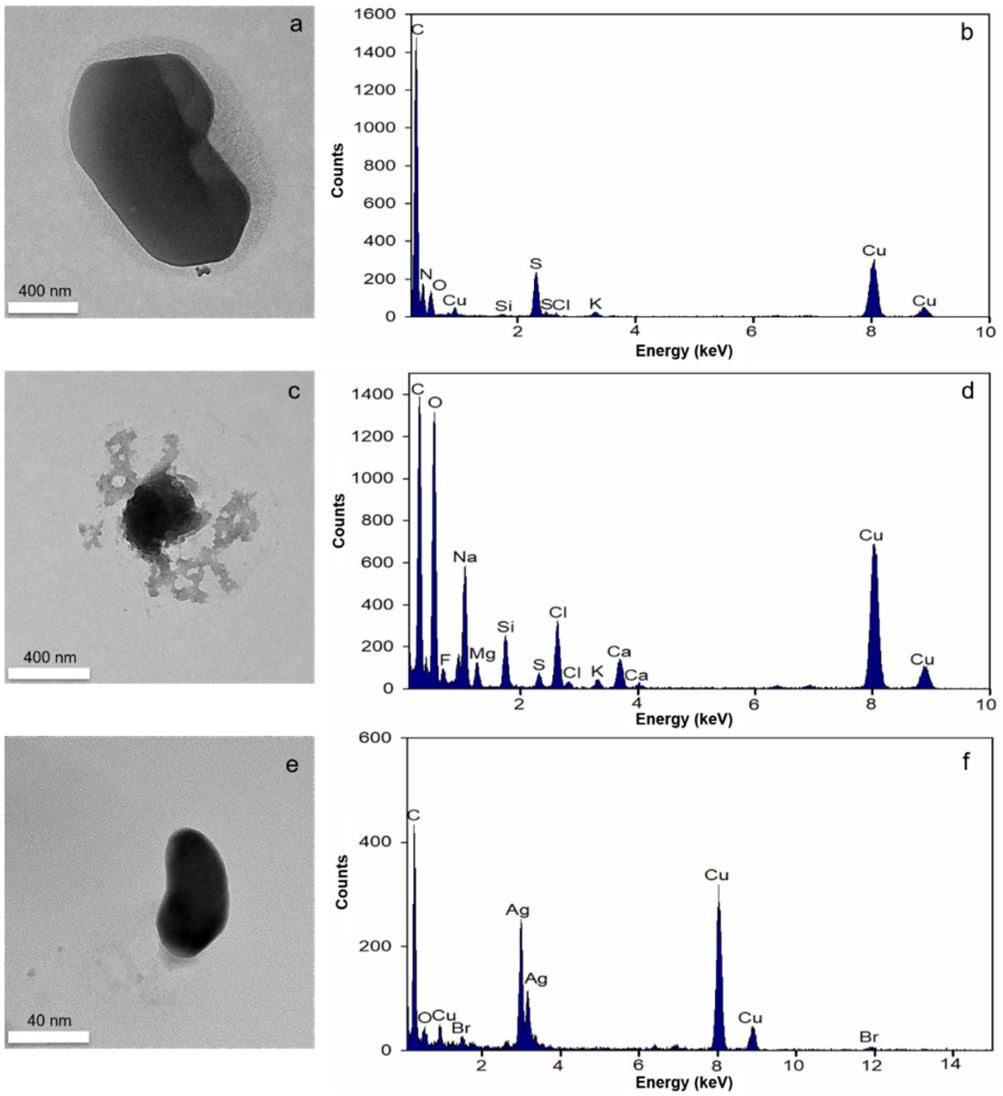

Figure 6. Electron microscopy images with energy-dispersive X-ray spectroscopy (EDS) of particles collected from loaded Cl2-RPGE (Cl2 Reactive Phase Gas Extraction) tubes. (**a**,**b**) Demonstrate Cl on a rigid particle, (**c**,**d**) Indicate possible presence of calcium carbonate with Cl present, and (**e**,**f**) Show the identification of Br presence. The Cu signals are due to the 400 mesh Cu grid used as a substrate.

4. Discussion

When a comparison is drawn between the current work's measurements and the long-term NAPS data set, it is observed that the yearly trend is continued. This is demonstrated in Figure 7, which overlaps the long-term NAPS chloride plot with the current work's photolabile chlorine measurements.

The peak concentrations of particulate chloride occur between the months of January and March of each year, with the current work results in agreement for the one winter period of 2019. This agreement occurs despite the fact that the NAPS chloride data are only generated from $PM_{2.5}$ particulates, whereas the current work measures gaseous photolabile chlorine. Deposited road dust and road salt could be very significant sources of chlorine via heterogeneous chemical pathways, along with suspended chloride in aerosols, especially in a high surface area urban environment.

A comparison can also be drawn between the current work's methods and the more traditional methods employed in previous studies. Table 1 compares the results of the current study with a number of previous studies, which utilized well-established instrumental methods. It includes the common methods that have been used for Cl_2 and other photolabile halogen species, type of measurement

method, and observation results. In order to compare values for the detection limit and measured range of values, the values for our study were converted to ppt using the approximation that a significant portion of our measurements were due to Cl_2. This technique was also calibrated for Cl_2. When the detection limit of 0.9 ng/m^3 and maximum value of 545 ng/m^3 are converted, we obtain 0.3 ppt and 188 ppt, respectively. As shown in Table 1, the approximate observation range for this study in ppt is within the range of selected previous tropospheric sampling.

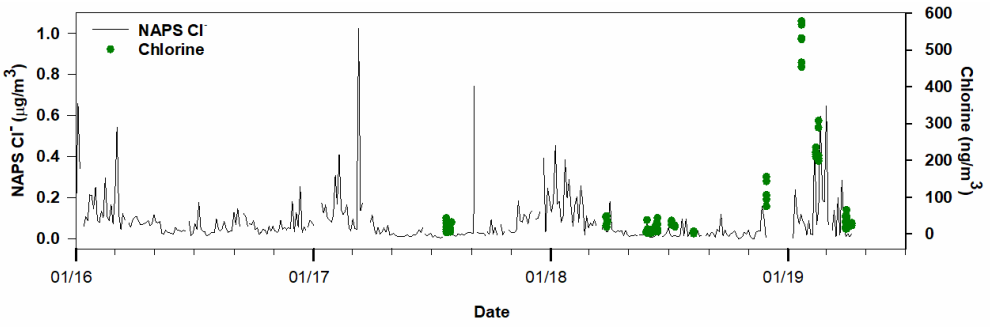

Figure 7. Time series of NAPS data showing the 2016–2019 trend for Cl^- from $PM_{2.5}$ measurements, and the comparison with photolabile chlorine measurements during overlapped periods.

It is noteworthy that the measured concentrations of photolabile halogens reported in this study are averages over a period of time (30 min). The data presented in Table 1 are from studies that employ real-time sampling such as with APCI-MS/MS, resulting in very high temporal resolution in comparison to the integrated sampling of the current work. The disadvantages of integrated sampling may be minimized by adjusting the sampling period and rate depending on the ambient concentrations being measured to optimize the temporal resolution and signal. In contrast, this method can have much higher spatial resolution, since the interfaces are miniaturized and easy to operate, which is advantageous for sampling multiple locations simultaneously. Remote data collection can be further included in the automation of this unit.

It must be noted that most studies tabulated in Table 1 are in polar regions, marine boundary layers, salt lakes, or coastal areas, which have access to natural salt sources. During the last three decades, it has become increasingly clear that through several photochemical species, halogen activations can take place. In these mechanisms, chloride in salts becomes a more reactive species such as Cl atoms directly or precursors of chlorine atoms such as HOCl or BrCl [32].

Yet, Montreal is a river island, which does not receive a significant amount of natural salt. However, there are various anthropogenic sources of salts in the city, most notably during the snow removal processes, which can last up to 5 months per year. Indeed, Montreal receives on average approximately 2.1 m of snow per year in comparison to Moscow, which receives approximately 1.2 m/yr. This demonstrates that even compared to another cold-climate metropolitan city, Montreal is an ideal location for this study due to the possible additional cycles of salt, snow melt, and precipitation. To remove snow, the City of Montreal uses 140,000 tons of salt per year [33]. Hence, we show evidence that halogen activation on natural and anthropogenic urban surfaces and on airborne particles can be efficient in the activation of halogens, as has been previously discussed [10,18–20]. The results of this research indicate clearly that the highest chloride content was consistently observed during the winter, and the trends observed in this work agree with a recent study that demonstrated that road salt aerosols could be a primary source of $ClNO_2$ generation [19]. The pathway for this production depends on the presence of NO_x and O_3. It begins with the reaction of NO_2 and O_3 to produce NO_3 and O_2. NO_3 can react with NO_2 to produce N_2O_5, which is the compound that can react with particulate-based chloride to generate $ClNO_2$ [19,34,35]. The last step of this reaction process is complex, as it involves a multistep process in the aqueous phase of an aerosol [35]. Therefore, it is influenced by humidity as well for both controlling the disproportionation of N_2O_5 in the aqueous phase, but also the concentration of other

species (such as organics, etc.) in the aqueous phase. This is relevant because the concentration of other species may either enhance or suppress the uptake of N_2O_5 into the aqueous phase and therefore affect the production of $ClNO_2$ that is released upon sunlight [35]. Then, the photolysis of $ClNO_2$ during the daytime produces a large amount of chlorine atoms. While we see an increase in our measurements that may correspond to this proposed mechanism, our current setup might not completely capture all released chlorine atoms due to possible line loss. Note that several blank runs with pure air were performed between the experiments through the same tube, and we did not see any GC-MS signals above baseline. When this work's detection limit is approximated as 0.3 ppt for Cl_2 for the described 30 min sampling at 1 LPM, it compares well with the previous studies in Table 1, demonstrating the potential of the Cl2-RPGE tube method. The approximated maximum value of 188 ppt as Cl_2 shows that our measurements were the same order of magnitude as previous measurements in polluted urban sites.

Table 1. Comparison of the current study with selected previous halogen studies, indicating study, analyte, method, and range of mixing ratios from the detection limit to the highest recorded measurement. Shading indicates sample region type as marine boundary layer (gray), polar (blue), and influenced by urban locations (orange). Montreal data are depicted in the last row in bold for the purpose of clarity. APCI-MS: atmospheric pressure chemical ionization mass spectrometry, DOAS: differential optical absorption spectroscopy, CI-MS/MS: chemical ionization mass spectrometry.

Location and Date	Analyte of Interest	Detection Method	Detection Limit to Highest Recorded Measurement	References
Marine BL Eastern Long Island, NY, June 1996	Cl_2	APCI-MS/MS	15–150 pptv	[21]
Great Salt Lake UT, October 2000	ClO	DOAS	4–15 pptv	[22]
Marine BL La Jolla, CA, January 2006	Cl_2	APCI-MS/MS	1–26 pptv	[23]
Marine BL Cape Verde Atmospheric Observatory, June 2009	Cl_2	CI-MS/MS	1–35 pptv	[24]
Polar BL ALERT, 1995	Photolyzable chlorine (Cl_2, HOCl, etc)	Photolyzable halogen detector, with GC coupled to electron capture detector	9–100 pptv	[25]
Polar BL ALERT, 2000	Cl_2	APCI-MS/MS	2 pptv–Not detected	[26]
Polar BL Barrow, AK, Spring 2009	Cl_2	CI-MS	1.1–400 pptv	[27]
Coastal Urban Air Irvine, CA, Fall 2005	Cl_2	APCI-MS/MS	2.5–20 pptv	[28]
Polluted Coastal Region Los Angeles basin, CalNex 2010 field study	Cl_2	CI-MS	<2–200 pptv	[29]
Calgary, AB, Canada, Spring 2010	$ClNO_2$	CI-MS	5–250 pptv	[10]
Calgary, AB, Canada, Spring 2011	$ClNO_2$	CI-MS	5–338 pptv	[11]
Kleiner Feldberg, southwestern Germany, Summer 2011	$ClNO_2$	CI-MS	3–800 pptv	[30]
Eastern United States, Winter 2015	$ClNO_2$	I-ToF-CIMS	0.6–119 pptv	[31]
Montreal, 2017–2019	**Photolabile chlorine (Cl_2, HOCl, etc)**	**Cl2-RPGE tube coupled to GC-MS**	**0.9–545 ng/m^3 (0.3–188 ppt as Cl_2)**	**This Study**

5. Conclusions and Future Studies

This study presents a decade of chloride ion $PM_{2.5}$ measurements (2010–2019) along with a suite of atmospheric pollutants (such as NO_x, O_3) and of intermittent atmospheric photolabile chlorine

during the summers of 2017, 2018, and winter of 2019 in the northern urban environment of Montreal, Canada using Cl2-RPGE tubes coupled with GC-MS for analysis. This research presents a systematic long-term study of chloride in $PM_{2.5}$ in a large metropolitan urban setting. These data are significant in future modeling as they provides a long-term data set with hints to the impacts of anthropogenic chlorine activation on the oxidation potential of the atmosphere in a cold-climate urban environment, due to anthropogenic salt, which can affect the urban oxidation photochemical processes. We conclude over the period of 10 years that the highest chloride ion concentrations in $PM_{2.5}$ particulates occur every year during the wintertime in Montreal. This is the period in which the City of Montreal adds about 140,000 tons of salts (NaCl and $CaCl_2$) as a de-icing agent every year, which is thereby anthropogenic. The measurement of photolabile chlorine during the overlapping year demonstrates that the highest photolabile chlorine is observed during the same period, hinting that chloride ions have been transformed to more reactive photolabile chlorine species. Yet, further detailed modeling studies will be required to validate it for cold-climate urban regions. The activation processes of reactive chlorine from chloride have been the subject of numerous studies in the literature [12,32]. It has also been significantly modeled for various regions of the globe from the marine boundary layer, to Arctic, Antarctica, and salt lakes [12]. Interestingly, a recent modeling study has suggested that including halogens in the models will result in a decrease in ozone concentration [36] and thus change the oxidation potential of the troposphere. This study can be expanded upon in future studies utilizing the more efficient photolysis setup. It would also be beneficial to expand upon the presented work to quantify photolabile bromine in the future. S/TEM-EDS results indicate the presence of atmospheric bromine, and atmospheric bromine species may be detectable with this sorbent method as well upon modification of sampling conditions. Further experiments are required to optimize the efficiency of the Cl2-RPGE tubes for the quantitative measurement of both photolabile chlorine and bromine species. Field sampling from multiple sites would also demonstrate the high spatial resolution of the presented method and could serve as a platform for identifying point sources of halogens in and around urban Montreal or other more polluted regions. Lastly, we propose further modeling, specifically snow-air coupled models, of such processes for cold-climate urban environments, the influences of the boundary layer meteorology, snow–air interactions, and the impact on atmospheric oxidation processes.

Supplementary Materials: The following are available online at http://www.mdpi.com/2073-4433/11/8/812/s1, Figure S1: Image of Cl2-RPGE tube, Figure S2: Representative calibration plots, Table S1: Tabulated parameters identifying lower limits of the sampling method, Table S2: Method accuracy with spike and recovery of 50 ppt, Table S3: Method accuracy with spike and recovery of 5 ppt, Table S4: Method repeatability over six 50 ppt samples, Table S5: Method intermediate precision determination day 1, Table S6: Method intermediate precision determination day 2, Table S7: Method intermediate precision determination day 3, Figure S3: Simplified setup diagram, Figure S4: Comparison of UV lamp wavelengths to absorption wavelengths for selected relevant molecules, Section S5: Sources of uncertainty, Figure S5: Solar irradiance spectrum, Figure S6: Time series plots of Cl^-/CO, O_3/CO, NO_x/CO, and $PM_{2.5}$/CO concentration ratios, Figure S7: Time series of O_3 and NO_x concentration product and seasonality, Figure S8: Time series of O3 and NOx product concentrations divided by CO, Figure S9: Representative SIM chromatogram of calibration standard, and Figure S10: Representative SIM chromatogram of sample.

Author Contributions: Conceptualization, P.A.A.; Formal analysis, R.H.; Funding acquisition, P.A.A.; Investigation, R.H., O.N. and E.N.; Methodology, R.H. and O.N.; Resources, O.N. and P.A.A.; Supervision, P.A.A.; Validation, R.H., O.N. and E.N.; Writing—original draft, R.H.; Writing—review and editing, O.N. and P.A.A. All authors have read and agreed to the published version of the manuscript.

Funding: This research was funded by The Natural Sciences and Engineering Council of Canada (NSERC), HydroQuebec, Environment and Climate Change Canada (ECCC), The Fonds de recherché du Quebec–Nature et technologies (FRQNT), and McGill University.

Acknowledgments: We would like to thank Hannah Szeptycki and Emma Morris for assistance during some sampling periods, and David Liu from the facility for electron microscopy research at McGill University for running our samples with the FEI Tecnai G2F20 S/TEM microscope. We are grateful to colleagues from the City of Montreal (Sonia Melancon and Fabrice Godefroy) for generously sharing their recently validated data, and Ashu Dastoor (ECCC) for intellectually exciting discussions. We would also like to thank fellow group member Devendra Pal for assistance with the use of data processing software.

Conflicts of Interest: The academic authors declare no conflict of interest.

References

1. Saiz-Lopez, A.; von Glasow, R. Reactive halogen chemistry in the troposphere. *Chem. Soc. Rev.* **2012**, *41*, 6448–6472. [CrossRef] [PubMed]
2. Faxon, C.B.; Allen, D.T. Chlorine chemistry in urban atmospheres: A review. *Environ. Chem.* **2013**, *10*, 221–233. [CrossRef]
3. Simpson, W.R.; Brown, S.S.; Saiz-Lopez, A.; Thornton, J.A.; von Glasow, R. Tropospheric halogen chemistry: Sources, cycling, and impacts. *Chem. Rev.* **2015**, *115*, 4035–4062. [CrossRef] [PubMed]
4. Wang, X.; Jacob, D.J.; Eastham, S.D.; Zhu, L.; Chen, Q.; Alexander, B.; Sherwen, T.; Evans, M.J.; Lee, B.H.; Haskins, J.D.; et al. The role of chlorine in global tropospheric chemistry. *Atmos. Chem. Phys.* **2019**, *19*, 3981–4003. [CrossRef]
5. Ariya, P.A.; Khalizov, A.F.; Gidas, A. Reaction of gaseous mercury with atomic and molecular halogens: Kinetics, product studies, and atmospheric implications. *J. Phys. Chem. A* **2002**, *106*, 7310–7320. [CrossRef]
6. Simpson, W.R.; von Glasow, R.; Riedel, K.; Ariya, P.; Bottenheim, J.; Burrows, J.; Carpenter, L.J.; Frieß, U.; Goodsite, M.E.; Heard, D.; et al. Halogens and their role in polar boundary-layer ozone depletion. *Atmos. Chem. Phys.* **2007**, *7*, 4375–4418. [CrossRef]
7. Atkinson, R.; Baulch, D.L.; Cox, R.A.; Crowley, J.N.; Hampson, R.F.; Hynes, R.G.; Jenkin, M.E.; Rossi, M.J.; Troe, J.; Wallington, T.J. Evaluated kinetic and photochemical data for atmospheric chemistry: Volume IV—gas phase reactions of organic halogen species. *Atmos. Chem. Phys.* **2008**, *8*, 4141–4496. [CrossRef]
8. Ravishankara, A.R. Are chlorine atoms significant tropospheric free atoms? *Proc. Natl. Acad. Sci. USA* **2009**, *106*, 13639–13640. [CrossRef]
9. Young, C.J.; Washenfelder, R.A.; Edwards, P.M.; Parrish, D.D.; Gilman, J.B.; Kuster, W.C.; Mielke, L.H.; Osthoff, H.D.; Tsai, C.; Pikelnaya, O.; et al. Chlorine as a primary radical: Evaluation of methods to understand its role in initiation of oxidative cycles. *Atmos. Chem. Phys.* **2014**, *14*, 3427–3440. [CrossRef]
10. Mielke, L.H.; Furgeson, A.; Osthoff, H.D. Observation of $ClNO_2$ in a mid-continental urban environment. *Environ. Sci. Technol.* **2011**, *11*, 8889–8896. [CrossRef]
11. Mielke, L.H.; Furgeson, A.; Odame-Ankrah, C.A.; Osthoff, H.D. Ubiquity of $ClNO_2$ in the urban boundary layer of Calgary, Alberta, Canada. *Can. J. Chem.* **2016**, *94*, 414–423. [CrossRef]
12. Finlayson-Pitts, B.J. Halogens in the troposphere. *Anal. Chem.* **2010**, *82*, 770–776. [CrossRef] [PubMed]
13. Fang, X.; Park, S.; Saito, T.; Tunnicliffe, R.; Ganesan, A.L.; Rigby, M.; Li, S.; Yokouchi, Y.; Fraser, P.J.; Harth, C.M.; et al. Rapid increase in ozone-depleting chloroform emissions from China. *Nat. Geosci.* **2018**, *12*, 89–93. [CrossRef]
14. Thornton, J.A.; Kercher, J.P.; Riedel, T.P.; Wagner, N.L.; Cozic, J.; Holloway, J.S.; Dubé, W.P.; Wolfe, G.M.; Quinn, P.M.; Middlebrook, A.M.; et al. A large atomic chlorine source inferred from mid-continental reactive nitrogen chemistry. *Nature* **2010**, *464*, 271–274. [CrossRef] [PubMed]
15. Environment and Climate Change Canada NAPS Data Portal. Available online: http://maps-cartes.ec.gc.ca/rnspa-naps/data.aspx (accessed on 4 May 2020).
16. Kolesar, K.R.; Mattson, C.N.; Peterson, P.K.; May, N.W.; Prendergast, R.K.; Pratt, K.A. Increases in wintertime $PM_{2.5}$ sodium and chloride linked to snowfall and road salt application. *Atmos. Environ.* **2018**, *177*, 195–202. [CrossRef]
17. Poulain, A.J.; Garcia, E.; Amyot, M.; Campbell, P.G.C.; Raofie, F.; Ariya, P. Biological and chemical redox transformations of mercury in fresh and salt waters of the high Arctic during spring and summer. *Environ. Sci. Technol.* **2007**, *41*, 1883–1888. [CrossRef]
18. Poulain, A.J.; Lalonde, J.D.; Amyot, M.; Shead, J.A.; Raofie, F.; Ariya, P.A. Redox transformations of mercury in an Arctic snowpack at springtime. *Atmos. Environ.* **2004**, *38*, 6763–6774. [CrossRef]
19. McNamara, S.M.; Kolesar, K.R.; Wang, S.; Kirpes, R.M.; May, N.W.; Gunsch, M.J.; Cook, R.D.; Fuentes, J.D.; Hornbrook, R.S.; Apel, E.C.; et al. Observation of road salt aerosol driving inland wintertime atmospheric chemistry. *ACS Cent. Sci.* **2020**, *6*, 684–694. [CrossRef]
20. Riedel, T.P.; Wagner, N.; Dubé, W.P.; Middlebrook, A.M.; Young, C.J.; Öztürk, F.; Bahreini, R.; VandenBoer, T.; Wolfe, D.E.; Williams, E.J.; et al. Chlorine activation within urban or power plant plumes: Vertically resolved $ClNO_2$ and Cl_2 measurements from a tall tower in a polluted continental setting. *J. Geophys. Res. Atmos.* **2013**, *118*, 8702–8715. [CrossRef]

21. Spicer, C.W.; Chapman, E.G.; Finlayson-Pitts, B.J.; Plastridge, R.A.; Hubbe, J.M.; Fast, J.D.; Berkowitz, C.M. Unexpectedly high concentrations of molecular chlorine in coastal air. *Nature* **1998**, *394*, 353–356. [CrossRef]
22. Stutz, J.; Ackermann, R.; Fast, J.D.; Barrie, L. Atmospheric reactive chlorine and bromine at the Great Salt Lake, Utah. *Geophys. Res. Lett.* **2002**, *29*, 18-1–18-4. [CrossRef]
23. Finley, B.; Saltzman, E. Observations of Cl_2, Br_2, and I_2 in coastal marine air. *J. Geophys. Res. Atmos.* **2008**, *113*. [CrossRef]
24. Lawler, M.; Sander, R.; Carpenter, L.; Lee, J.; von Glasow, R.; Sommariva, R.; Saltzman, E. HOCl and Cl_2 observations in marine air. *Atmos. Chem. Phys.* **2011**, *11*, 7617–7628. [CrossRef]
25. Impey, G.; Shepson, P.; Hastie, D.; Barrie, L.; Anlauf, K. Measurements of photolyzable chlorine and bromine during the polar sunrise experiment 1995. *J. Geophys. Res. Atmos.* **1997**, *102*, 16005–16010. [CrossRef]
26. Spicer, C.W.; Plastridge, R.A.; Foster, K.L.; Finlayson-Pitts, B.J.; Bottenheim, J.W.; Grannas, A.M.; Shepson, P.B. Molecular halogens before and during ozone depletion events in the Arctic at polar sunrise: Concentrations and sources. *Atmos. Environ.* **2002**, *36*, 2721–2731. [CrossRef]
27. Liao, J.; Huey, L.G.; Liu, Z.; Tanner, D.J.; Cantrell, C.A.; Orlando, J.J.; Flocke, F.M.; Shepson, P.B.; Weinheimer, A.J.; Hall, S.R.; et al. High levels of molecular chlorine in the Arctic atmosphere. *Nat. Geosci.* **2014**, *7*, 91–94. [CrossRef]
28. Finley, B.D.; Saltzman, E.S. Measurement of Cl_2 in coastal urban air. *Geophys. Res. Lett.* **2006**, *33*, L11809. [CrossRef]
29. Riedel, T.P.; Bertram, T.H.; Crisp, T.A.; Williams, E.J.; Lerner, B.M.; Vlasenko, A.; Li, S.-M.; Gilman, J.; De Gouw, J.; Bon, D.M.; et al. Nitryl chloride and molecular chlorine in the coastal marine boundary layer. *Environ. Sci. Technol.* **2012**, *46*, 10463–10470. [CrossRef]
30. Phillips, G.J.; Tang, M.J.; Thieser, J.; Brickwedde, B.; Schuster, G.; Bohn, B.; Lelieveld, J.; Crowley, J.N. Significant concentrations of nitryl chloride observed in rural continental Europe associated with the influence of sea salt chloride and anthropogenic emissions. *Geophys. Res. Lett.* **2012**, *39*. [CrossRef]
31. McDuffie, E.E.; Fibiger, D.L.; Dubé, W.P.; Hilfiker, F.L.; Lee, B.H.; Jaeglé, L.; Guo, H.; Weber, R.; Reeves, J.M.; Weinheimer, A.J.; et al. $ClNO_2$ yields from aircraft measurements during the 2015 WINTER campaign and critical evaluation of the current parameterization. *J. Geophys. Res. Atmos.* **2018**, *123*, 12994–13015. [CrossRef]
32. Ariya, P.A. Mid-latitude mercury loss. *Nat. Geosci.* **2011**, *4*, 14–15. [CrossRef]
33. Montreal Municipal Web Site. Available online: http://ville.montreal.qc.ca/snowremoval/operations-delais (accessed on 4 May 2020).
34. Roberts, J.M.; Osthoff, H.D.; Brown, S.S.; Ravishankra, A.R. N_2O_5 oxidizes chloride to Cl_2 in acidic atmospheric aerosol. *Science* **2008**, *321*, 1059. [CrossRef] [PubMed]
35. Phillips, G.J.; Thieser, J.; Tang, M.; Sobanski, N.; Schuster, G.; Fachinger, J.; Drewnick, F.; Borrmann, S.; Bingemer, H.; Lelieveld, J.; et al. Estimating N_2O_5 uptake coefficients using ambient measurements of NO_3, $N2O_5$, $ClNO_2$ and particle-phase nitrate. *Atmos. Chem. Phys.* **2016**, *16*, 13231–13249. [CrossRef]
36. Sherwen, T.; Evans, M.J.; Sommariva, R.; Hollis, L.D.J.; Ball, S.M.; Monks, P.S.; Reed, C.; Carpenter, L.J.; Lee, J.D.; Forster, G.L.; et al. Effects of halogens on European air-quality. *Faraday Discuss.* **2017**, *200*, 75–100. [CrossRef] [PubMed]